

DISCOVERY OF FAR-INFRARED PURE ROTATIONAL TRANSITIONS OF CH⁺ IN NGC 7027¹

J. CERNICHARO

Consejo Superior de Investigaciones Científicas, Instituto de Estructura de la Materia, Departamento Física Molecular, Serrano 123, E-28006 Madrid, Spain

X.-W. LIU

Department of Physics and Astronomy, University College London, Gower Street, London WC1E 6BT, England, UK

E. GONZÁLEZ-ALFONSO

Universidad de Alcalá de Henares, Departamento Física, Campus Universitario, E-28871 Alcalá de Henares, Spain; and Observatorio Astronómico Nacional, E-28800, Alcalá de Henares, Madrid, Spain

P. COX

Institut d'Astrophysique Spatiale, Bâtiment 121, Université de Paris XI, F-91405 Orsay Cedex, France

M. J. BARLOW

Department of Physics and Astronomy, University College London, Gower Street, London WC1E 6BT, England, UK

T. LIM

The LWS Instrument—Dedicated Team, ISO Science Operations Centre, P.O. Box 50727, E-28080 Madrid, Spain

AND

B. M. SWINYARD

Rutherford Appleton Laboratory, Chilton, Didcot, Oxon OX11 0QX, England, UK

Received 1997 March 4; accepted 1997 April 17

ABSTRACT

We report the discovery of the rotational spectrum of CH⁺ in the *Infrared Space Observatory* Long Wavelength Spectrometer (LWS) spectrum of the planetary nebula NGC 7027. The identification relies on a 1996 reanalysis of the LWS spectrum by Liu et al. and on new LWS data. The strong line at 179.62 μm (coinciding with the $2_{12}-1_{01}$ transition of water vapor) and the lines at 119.90 and 90.03 μm (reported as unidentified by Liu et al.), whose frequencies are in the harmonic relation 2:3:4, are shown to arise from the $J = 2-1$, $3-2$, and $4-3$ rotational transitions of CH⁺. This identification is strengthened by the new LWS spectra of NGC 7027, which clearly show the next two rotational lines of CH⁺ at 72.140 and 60.247 μm . This is the first time that the pure rotational spectrum of CH⁺ has been observed. This discovery opens the possibility of probing the densest and warmest zones of photodissociation regions. We derive a rotational temperature for the CH⁺ lines of 150 ± 20 K and a CH⁺/CO abundance ratio of $2-6 \times 10^{-4}$.

Subject headings: planetary nebulae; individual (NGC 7027) — infrared: ISM: lines and bands

1. INTRODUCTION

The spectrometers on board the *Infrared Space Observatory* (ISO) provide a unique opportunity to study important molecular species through transitions that are inaccessible from the ground or from airborne platforms. This has been illustrated by the recent ISO results on the thermal lines of water vapor. Water vapor has been measured in high abundance [$x(\text{H}_2\text{O}) \approx 10^{-5}$] in star-forming regions and evolved stars using both the Short Wavelength Spectrometer (SWS) and the Long Wavelength Spectrometer (LWS) (e.g., van Dishoeck & Helmich 1996; Barlow et al. 1996; Cernicharo et al. 1997; Cox et al. 1997). The detection of water vapor (together with OH) was also reported by Liu et al. (1996, hereafter L96) in the LWS spectrum of the planetary nebula NGC 7027. This was an unexpected result because NGC 7027 is a carbon-rich source.

In this Letter, we rediscuss the previous identification of the water vapor emission lines in the LWS spectrum of NGC 7027. The 179.53 μm line together with two lines at 119.89 μm (near the OH 119.3 μm doublet) and 90.07 μm , both unidentified in

L96, are now shown to arise from the pure rotational spectrum of CH⁺. We also present new ISO LWS data that show two further rotational lines of CH⁺ and confirm the previous detection of OH and probably also of H₂O.

2. IDENTIFICATION OF CH⁺

The identification of water vapor in NGC 7027 by L96 relies mainly on the observation of a strong line at 179.56 μm coinciding with the 179.53 μm H₂O rotational $2_{12}-1_{01}$ transition. Two other features quoted as possible water lines in L96 were flagged as “identification questionable.” In addition to the H₂O line, L96 also reported the detection of OH through the 119.3 μm fundamental transition. This line is blended with an equally strong feature at 119.89 μm , which remained unidentified. Two other OH lines (at 79.2 and 84.5 μm) were tentatively reported.

L96 also reported a strong unidentified line at 90.07 μm . We note that the wavelengths of the lines at 179.56, 119.89, and 90.07 μm are nearly in the harmonic relation 2:3:4. Assuming that the 179.56 μm line does not arise from water vapor but instead that the three lines arise from another molecular carrier, these lines could correspond to the rotational transitions $J = 2-1$, $3-2$, and $4-3$ of a linear molecule. From the

¹ Based on observations with ISO, an ESA project with instruments funded by ESA Member States (especially the Principal Investigator countries: France, Germany, the Netherlands, and the United Kingdom) and with the participation of ISAS and NASA.

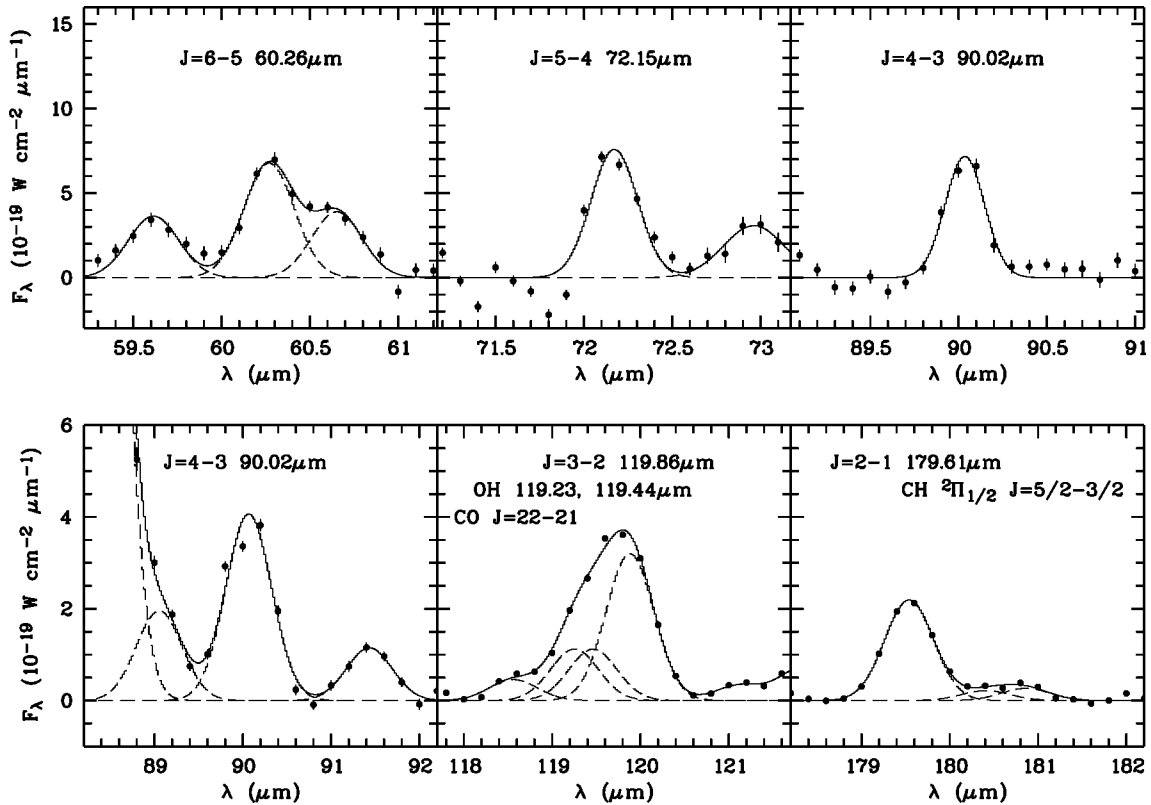


FIG. 1.— CH^+ lines observed in NGC 7027 (the continuum has been subtracted from the data). The solid lines are Gaussian line profile fits to the observed features (for blends, contributions from individual components are shown as dashed lines). The $J = 2-1$ line at $179.62 \mu\text{m}$ was previously assigned to H_2O . For the $J = 4-3$ line, spectra from two different detectors—LW1 (*bottom panel*; the sharp rise at short wavelengths is due to the strong $[\text{O III}]$ $88.36 \mu\text{m}$ line) and SW5 (*upper panel*)—are shown. The $J = 4-3$ line is blended with the $J = 29-28$ line of CO at $90.16 \mu\text{m}$, which could contribute with an intensity less than $10^{-19} \text{ W cm}^{-2}$ —the $J = 27-26$ and $J = 26-25$ lines of CO can be seen in the bottom left-hand panel of Fig. 2 with intensities of $\sim 10^{-19} \text{ W cm}^{-2}$. The lines at 59.5 and $60.7 \mu\text{m}$ in the top left-hand panel are unknown.

three lines we derive the following rotational constants for the carrier: $B = 13.95 \pm 0.03 \text{ cm}^{-1}$ and $D = 0.0017 \pm 0.0005 \text{ cm}^{-1}$ (1σ errors). The observed frequencies and inferred rotational constants indicate that the carrier must be diatomic and should contain a hydrogen atom. The rotational constants are comparable to those of CH ($B = 14.19 \text{ cm}^{-1}$, $D = 0.0014 \text{ cm}^{-1}$) and show an excellent agreement with those of the CH^+ ion ($B = 13.9302 \text{ cm}^{-1}$ and $D = 0.0014 \text{ cm}^{-1}$; Carrington & Ramsay 1982).

Prompted by the observation of three lines in harmonic relation that are consistent with CH^+ , we have processed all the ISO LWS01 grating spectra of NGC 7027 so far obtained up to ISO revolution 377, in an effort to detect the $J = 5-4$ and $6-5$ transitions of CH^+ , which are predicted at wavelengths of 72.15 and $60.26 \mu\text{m}$ and were not detected by L96. In total, there are nine separate observations, each covering a wavelength range from 43 to $195 \mu\text{m}$, obtained during revolutions 27, 39, 342, 349, 356, 363, and 377. All the data were calibrated using Version 6 of the Off-Line Processing package (OLP). The observation from revolution 27 consists of three scans, with two 0.5 s integration ramps at each grating position, sampled at $1/4.5$ of a spectral resolution element, the latter being $0.3 \mu\text{m}$ for the SW1–SW5 detectors ($\lambda < 93 \mu\text{m}$) and $0.6 \mu\text{m}$ for the LW1–LW5 detectors ($\lambda > 84 \mu\text{m}$). Each of the five observations obtained between revolutions 342 and 377 consists of six scans with one 0.5 s ramp at each grating position, sampled at $1/9$ of a resolution element. Three observations were obtained in revolution 39. Each consists of

five scans with two 0.5 s ramps at each grating position, sampled at $1/15$ of a resolution element. The total on-target integration time was $23,930 \text{ s}$. The LWS has a circular aperture of diameter $85''$, significantly larger than the ionized or neutral regions of NGC 7027. The analysis presented in L96 was based on the three observations carried out in revolution 39, processed with Version 5 of the OLP. Although the current data have a total on-target time that is only 65% larger than that analyzed by L96, the final co-added spectrum has a much better S/N, by more than a factor of 2 in some wavelength regions, thanks to the much-improved instrumental filter profiles derived from additional observations of Uranus and the implementation of an algorithm that corrects for detector sensitivity drifts. The fluxes derived from the individual independent observations are in good agreement, and we estimate an accuracy of better than 20% for the absolute flux calibration.

Figure 1 shows the five CH^+ lines detected in our new spectra, including the two lines at 72.15 and $60.26 \mu\text{m}$, which are clearly detected in the present data. These five lines definitely establish the presence of CH^+ in NGC 7027. This is the first time that CH^+ is seen through its pure rotational spectrum. CH^+ , a common molecule in the diffuse interstellar medium, has been detected in the optical spectrum of only two evolved carbon-rich stars: in emission in the Red Rectangle, and in absorption in HD 213985 (Balm & Jura 1992; Hall et al. 1992; Waelkens et al. 1992; Bakker et al. 1997). Given the carbon-rich nature of NGC 7027 and the strong radiation field

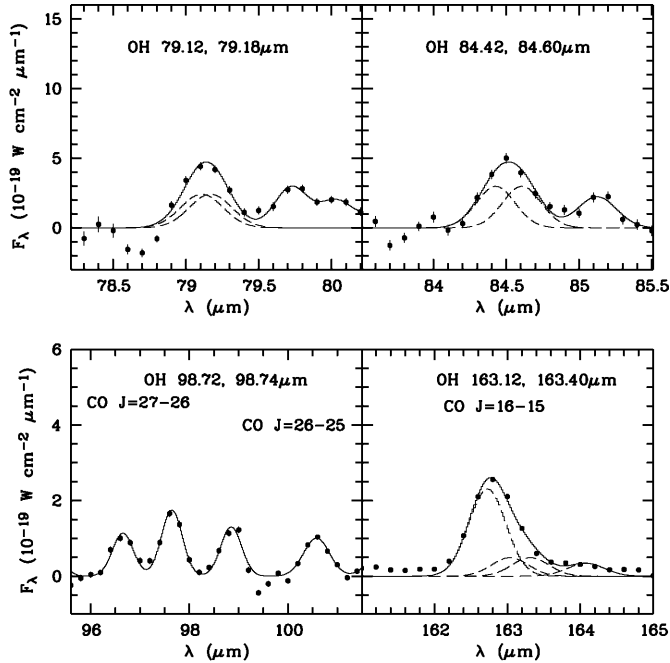


FIG. 2.—OH lines observed in NGC 7027 (after subtraction of the continuum). The OH 119.23, 119.44 μm lines, blending with the CH⁺ 119.86 μm line, are shown in the lower middle panel of Fig. 1. Due to the Λ -doubling, each of the OH transitions consists of two components, and two Gaussians of equal line width and intensity, having a central wavelength difference given by their laboratory values, were used to fit the line profiles, except for the 98.73 μm transition, which has a negligible wavelength splitting. Two lines in the bottom left-hand panel correspond to the $J = 27-26$ and $J = 26-25$ transitions of CO (at 96.77 and 100.46 μm , respectively), while the line at 97.6 μm in the same panel is unknown.

in its inner regions, it is thus not too surprising to find CH⁺ in this prototypical planetary nebula. In fact, soon after the detection of H₂ in NGC 7027 (Treffers et al. 1978), Black (1978) predicted that CH⁺, OH, and HeH⁺ might have detectable abundances in this nebula.

In addition, five OH lines are present (Fig. 2), confirming the previous detection of OH by L96. The CH⁺ and OH line fluxes are given in Table 1. Apart from the 179.6 μm line, two marginal features at 174.6 and 180.5 μm were tentatively assigned in L96 as possible water vapor lines. The 180.5 μm line is now shown to arise from CH (see Liu et al. 1997). However, the new data confirm the 174.6 μm line [$F = (1.44 \pm 0.17) \times 10^{-20} \text{ W cm}^{-2}$] and, in addition, show two lines at $108.05 \pm 0.1 \mu\text{m}$ [$F = (5.9 \pm 0.6) \times 10^{-20} \text{ W cm}^{-2}$] and $75.39 \pm 0.03 \mu\text{m}$ [$F = (6.6 \pm 2.5) \times 10^{-20} \text{ W cm}^{-2}$], coincident in wavelength with the $2_{21}-1_{10}$ (108.08 μm) and the $3_{21}-2_{12}$ (75.38 μm) lines of ortho-H₂O. Taking into account the density of lines and the lack of emission in the lines of para-water, the definitive assignment of these lines to water vapor will require high spectral resolution observations. No ¹³CH⁺ lines were detected in current spectrum. Finally, Figure 1 shows that the CH rotational line at 180.6 μm is much weaker than the nearby CH⁺ $J = 2-1$ line. A comparison of the observed intensities yields a CH⁺/CH abundance ratio of $\approx 5-10$ (see also Liu et al. 1997).

3. DISCUSSION

The line fluxes of Table 1 have been used to derive the rotational temperature, T_{rot} , of CH⁺. From a standard rota-

TABLE 1
CH⁺ AND OH LINE FLUXES FROM NGC 7027

λ_{obs} (μm)	Flux ^a	λ_{vac} (μm)	Transition
CH ⁺			
179.60 ± 0.04	1.51 ± 0.05	179.61	$J = 2-1$
119.88 ± 0.06	2.18 ± 0.17	119.86	$J = 3-2$
90.09 ± 0.06	2.64 ± 0.28	90.02	$J = 4-3^b$
90.02 ± 0.03	2.00 ± 0.22	90.02	$J = 4-3^c$
72.17 ± 0.03	2.50 ± 0.41	72.15	$J = 5-4$
60.27 ± 0.03	2.41 ± 0.33	60.26	$J = 6-5$
OH			
119.36 ± 0.06	1.53 ± 0.11	119.34	${}^2\Pi_{3/2}J = 5/2-3/2^d$
84.50 ± 0.02	1.98 ± 0.15	84.51	${}^2\Pi_{3/2}J = 7/2-5/2$
	<2.4 (3 σ)	65.20	${}^2\Pi_{3/2}J = 9/2-7/2$
163.23 ± 0.08	0.62 ± 0.07	163.26	${}^2\Pi_{1/2}J = 3/2-1/2^e$
98.85 ± 0.10	0.69 ± 0.12	98.73	${}^2\Pi_{1/2}J = 5/2-3/2$
79.12 ± 0.04	1.76 ± 0.23	79.15	${}^2\Pi_{1/2-3/2}J = 1/2-3/2$

^a In $10^{-19} \text{ W cm}^{-2}$.

^b LW1 detector.

^c SW5 detector.

^d Blended with CH⁺ $J = 3-2$.

^e Blended with CO $J = 16-15$.

tional analysis, in which we assume a uniform rotational temperature for all the rotational levels of CH⁺, we obtain $T_{\text{rot}} \approx 150 \pm 20 \text{ K}$ (see Fig. 3) and a CH⁺ total column density of 2.5×10^{17} . It is worth noting that similar CH⁺ rotational temperatures were derived from optical observations in the Red Rectangle and in HD 213985 by Bakker et al. (1997), i.e., 202 and 155 K, respectively. A similar rotational analysis for the CO line fluxes given by L96 yields a rotational temperature for CO of 240 K and a total number of CO molecules $\approx 10^{21}$. Assuming that the molecular emission of both species arises from the same region, we obtain a CH⁺/CO abundance ratio of 2×10^{-4} . Assuming that the size of the photodissociation region (PDR) in NGC 7027 is about 6'', we derive a column density for CH⁺ of $8 \times 10^{13} \text{ cm}^{-2}$.

In order to estimate the physical conditions needed to

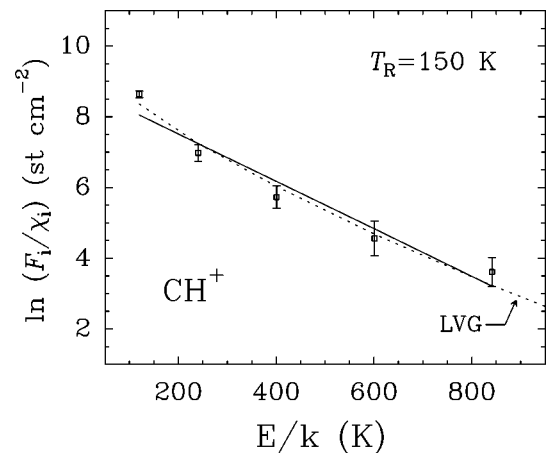


FIG. 3.—Rotational temperature analysis for CH⁺ in NGC 7027. The ordinates represent the natural logarithm of the observed fluxes (in W cm^{-2}) divided by $\chi_i \equiv (16 \times 10^{-7} \pi^3 v^4 \mu^2 J_{\text{up}})/(3c^3)$, where the symbols have the usual meaning and are in cgs units. The abscissa corresponds to the energy of the upper level of each rotational transition. The solid line represents the fit to the data assuming an uniform rotational temperature, while the dashed line represents the fluxes derived from the LVG models quoted in the text.

produce the observed CH^+ fluxes, we have made large velocity gradient (LVG) calculations that allow us to estimate the H_2 volume density and the CH^+ column density. Collisional cross sections for CH^+ with H_2 are not available, so we have used those of N_2H^+ (Green 1975). The values of the collisional cross sections for high kinetic temperatures were obtained from the N_2H^+ data available for 10–40 K by extrapolating the rate coefficients as the root square of the kinetic temperature. Typical estimates for the excitation rate coefficients are $\sim 10^{-10} \text{ cm}^3 \text{ s}^{-1}$. With a dipole moment of 1.68 D (e.g., Follmeg, Rosmus, & Werner 1987), the relevant critical H_2 densities for the $\text{CH}^+ J = 1$ level are on the order of $\sim 10^7 \text{ cm}^{-3}$. Even larger densities could be necessary to pump the high J levels (the $J = 6-5$ rotational transition has an Einstein coefficient for spontaneous emission of 1.9 s^{-1}) by collisions. For a distance of 700 pc (Hajian, Terzian, & Bignell 1993) and adopting a line width of 30 km s^{-1} , the observed CH^+ fluxes can be roughly explained with the following parameters: $n(\text{H}_2) = 2-5 \times 10^7 \text{ cm}^{-3}$, $T_K = 300-500 \text{ K}$, and a CH^+ column density of $2.5 \times 10^{14} \text{ cm}^{-2}$, which implies a CH^+/CO abundance ratio of $\approx 6 \times 10^{-4}$. The dashed line in Figure 3 shows the computed CH^+ line intensity fluxes for $n(\text{H}_2) = 5 \times 10^7 \text{ cm}^{-3}$ and $T_K = 300 \text{ K}$. An improved fit to the data could be obtained with a model where the low J transitions are excited in a region of moderate kinetic temperature and the high J levels are excited in a region with temperatures around 1000 K. But in any case, the density must be very high in order to explain the population of the $J = 4, 5$, and 6 rotational levels of CH^+ . The rotational lines of CH^+ could also be collisionally excited by impact of H and e^- . For collisions with e^- , $\gamma[J + 1 \rightarrow J]$ is approximately a few $\times 10^{-7} \text{ cm}^3 \text{ s}^{-1}$ for T_e between 100 and 1000 K (Dickinson & Flower 1981). Hence, electrons may compete with H_2 in populating the CH^+ rotational levels if $n_e/n(\text{H}) \sim 10^{-3}$, a condition reached only in the warm PDR, where all the carbon is in the form of C^+ . In this region, the H_2 densities quoted above could be lowered by a factor of 2–3 if collisions with e^- are taken into account. In addition, we must consider the possibility of excitation of the CH^+ rotational levels through absorption of photons in the ${}^1\Pi-{}^1\Sigma$ transition, followed by decay back to the ground state (in the Red Rectangle, the $\text{CH}^+ {}^1\Pi-{}^1\Sigma$ lines are observed in emission). Observations at optical wavelengths of CH^+ in NGC 7027 might provide important insights into the excitation mechanism of CH^+ . If such a pumping mechanism plays a role in the excitation of the rotational levels of CH^+ , then the densities necessary to explain the emission would be considerably lower.

The discrepancy between the CH^+/CO abundance ratio derived from the LVG calculations and that derived from the rotational analysis of the CH^+ lines arises from two facts: first, the assumptions in the rotational analysis that the CH^+ lines are optically thin (from the LVG calculations, the opacities are estimated to be $\approx 1-5$) and have a uniform rotational temperature and, second, from the uncertainties in the collisional cross sections used in the LVG models.

The formation of CH^+ via the reaction $\text{C}^+ + \text{H}_2 \rightarrow \text{CH}^+ + \text{H}$, which has an activation energy of $\sim 4000 \text{ K}$, requires a gas at high kinetic temperature ($\approx 1000 \text{ K}$). However, the present observations suggest that, in NGC 7027, the temperature of the region where CH^+ is emitted is much lower. In the interface region between the cold neutral gas and the fully ionized zone, a significant fraction of the H_2 population will be vibrationally excited, carrying an important part of the energy needed to activate the above reaction (Sternberg & Dalgarno 1995). A similar situation has been proposed by Jura, Turner, & Balm (1997) to explain the CH^+ emission in the Red Rectangle. For densities $10^6 < n(\text{H}_2) < 10^7 \text{ cm}^{-3}$, the formation rate of CH^+ could be high enough to produce column densities similar to those derived in this work, i.e., $0.8-2 \times 10^{14} \text{ cm}^{-2}$, as predicted in the models of Sternberg & Dalgarno (1995). However, if the density becomes too high, CH^+ might not survive because it will be rapidly destroyed by the reaction $\text{CH}^+ + \text{H}_2 \rightarrow \text{CH}_2^+ + \text{H}$. As in the diffuse interstellar medium, CH^+ could be formed efficiently in a region of moderate temperature in the presence of shocks with velocities of a few km s^{-1} . Low-velocity shocks have been observed in NGC 7027 (Jaminet et al. 1991) and should thus be taken into consideration in any detailed study of the formation and excitation of CH^+ in this planetary nebula.

The $\text{CH}^+ J = 2-1$ line can contaminate the LWS observations of water vapor at $179.5 \mu\text{m}$. The water line is seen in absorption toward several molecular clouds (Cernicharo et al. 1997; Cox et al. 1997) and arises from the ground level, while the possible absorption by CH^+ will arise from the $J = 1$ level, which is 40 K above the ground. Contamination of the H_2O $179.5 \mu\text{m}$ absorption line by CH^+ absorption is thus unlikely. However, the interpretation of the $179.6 \mu\text{m}$ line in emission in PDRs will require high spectral resolution data or the study of other transitions to disentangle the contributions of the H_2O and CH^+ lines.

REFERENCES

- Bakker, E. J., van Dishoeck, E. F., Waters, L. B. F. M., & Schoenmaker, T. 1997, *A&A*, in press
 Balm, S. P., & Jura, M. 1992, *A&A*, 261, L25
 Barlow, M. J., et al. 1996, *A&A*, 315, L241
 Black, J. H. 1978, *ApJ*, 222, 125
 Carrington, A., & Ramsay, D. A. 1982, *Physica Scripta*, 25, 272
 Cernicharo, J., et al. 1997, *A&A*, in press
 Cox, P., et al. 1997, *A&A*, in press
 Dickinson, A. S., & Flower, D. R. 1981, *MNRAS*, 196, 297
 Follmeg, B., Rosmus, P., & Werner, H.-J. 1987, *Chem. Phys. Lett.*, 136, 562
 Green, S. 1975, *ApJ*, 201, 366
 Hajian, A. R., Terzian, Y., & Bignell, C. 1993, *AJ*, 106, 1665
 Hall, D. I., Miles, J. R., Sarre, P. J., & Fossey, S. J. 1992, *Nature*, 358, 629
 Jaminet, P. A., Danchi, W. C., Sutton, E. C., Russell, A. P. G., Sandell, G., Bieging, J. H., & Wilner, D. 1991, *ApJ*, 380, 461
 Jura, M., Turner, J., & Balm, S. P. 1997, *ApJ*, 474, 741
 Liu, X.-W., et al. 1996, *A&A*, 315, L257 (L96)
 ———, 1997, *ApJ*, submitted
 Sternberg, A., & Dalgarno, A. 1995, *ApJS*, 99, 565
 Treffers, R. R., Fink, U., Larson, H. P., & Gautier, T. N., III. 1976, *ApJ*, 209, 793
 van Dishoeck, E. F., & Helmich, F. P. 1996, *A&A*, 315, L177
 Waalkens, C., van Winckel, H., Trams, N. R., & Waters, L. B. F. M. 1992, *A&A*, 256, L15